SERI/TP-211-2319
UC Category: 63
DE84004515

Electron Channeling and EBIC Studies of Polycrystalline Silicon Sheets

Y. S. Tsuo
R. J. Matson

May 1984

Presented at the
17th IEEE PV Specialists Conference
Orlando, Florida
1-5 May 1984

Prepared under Task No. 3434.10
FTP No. 462

Solar Energy Research Institute
A Division of Midwest Research Institute

1617 Cole Boulevard
Golden, Colorado 80401

Prepared for the
U.S. Department of Energy
Contract No. DE-AC02-83CH10093

Printed in the United States of America
Available from:
National Technical Information Service
U.S. Department of Commerce
5285 Port Royal Road
Springfield, VA 22161
Price:
Microfiche A01
Printed Copy A02

ELECTRON CHANNELING AND EBIC STUDIES OF POLYCRYSTALLINE SILICON SHEETS

Y. S. Tsuo and R. J. Matson

Solar Electric Research Division
Solar Energy Research Institute
1617 Cole Boulevard
Golden, Colorado 80401

ABSTRACT

Electron channeling and EBIC studies have been performed on silicon sheets grown by the edge-supported pulling (ESP) and low-angle silicon sheet (LASS) processes. We have found that the dominant grain structure of the ESP sheets is long, narrow grains with surface normals oriented near [011]; grains with this structure tend to have better electronic quality than random grains. We have also studied the twin-stabilized planar growth material of LASS sheets. This material, grown at 200 cm^2/min, is essentially single-crystal.

INTRODUCTION

We have used a combination of secondary electron imaging (SEI), electron channeling (1), and electron-beam-induced current (EBIC) line-scan and imaging (also known as charge collection scanning electron microscopy) (2) techniques in a scanning electron microscope (SEM) to correlate the morphology, crystallographic orientations, and the electronic quality of individual grains in polycrystalline silicon sheets. The high spatial resolution obtainable with electron channeling and EBIC techniques and the ability to select between the SEI, EBIC, and electron channeling modes in the SEM make them far superior to conventional structural and electrical characterization techniques for studying localized properties in polycrystalline semiconductors. We studied edge-supported pulling (ESP) silicon sheets grown at the Solar Energy Research Institute (SERI) and low-angle silicon sheets (LASS) grown at the Energy Materials Corporation (EMC) using these techniques. Defects in our silicon sheet samples were also studied using preferential etching followed by SEI or optical microscopy to complement information about electrically active defects gathered from EBIC studies. EBIC measurements were performed on Schottky (metal-semiconductor) barrier or diffused p-n junction devices on as-grown ESP samples that had been immersed in hydrofluoric acid to remove surface oxides and chemically polished in HNO_3/CH_3COOH/HF (3:2:2) for 2 minutes or less and on LASS samples in which the front surface had been mechanically lapped flat and then chemically-mechanically (Syton) polished on a polishing pad for about 30 minutes. These electron channeling studies can be performed on any sample or device surface that is not covered by metal contacts.

We generated a unit triangle electron channeling map for the electron channeling studies for silicon at 35 keV electron beam energy in the backscattered mode. This is similar to the silicon channeling map discussed in a recent review article by Joy et al. (1). We used a JEOL JSM 35C scanning electron microscope with a GW Electronics Model 130 backscattered electron detector and electronics to obtain electron channeling patterns (see, for example, Figure 5 in this paper). By comparing the electron channeling patterns of the silicon grains under study with the unit triangle map, we can readily identify the crystallographic orientations of the grains with an accuracy of better than 1^o. The same SEM system used to obtain electron channeling patterns and topographical images was also used to obtain EBIC area scans and EBIC line scans.

ESP SILICON SHEETS

In the ESP silicon sheet growth process (3-5), a capillary film of liquid silicon is formed between two parallel filaments (e.g., graphite) immersed in the liquid. As the filaments are pulled away from the melt, the remote region of the film solidifies between the filaments in a continuous fashion while the meniscus is replenished by capillarity. The high meniscus (about 7 mm in the mid-region) in the growth process contributes to enhanced grain size. However, the filaments, where the meniscus edges are pinned, serve as nucleation sites for grain growth during the solidification of the silicon. Consequently, a fine-grained structure exists within a few millimeters of the filaments, and larger longitudinal grains dominate the rest of the sheet (Figure 1). Grain widths on the order of 1 cm in the central region of the sheet can be achieved with seeded growth. But, to date, it is not known whether the effects of seeding can persist in continuous ESP sheet growth. For unseeded growth, although a fine-grained structure exists in the first few centimeters of sheet growth, large grains several millimeters wide with boundaries parallel to the growth direction often survive to extend down the silicon sheet and tend to block the spurious grains that nucleate from the sides. We have also observed that the average grain size of ESP silicon sheets tends to increase as the thickness of the crystal decreases (4).

All samples prepared for this study came from silicon sheets grown by the semicontinuous ESP

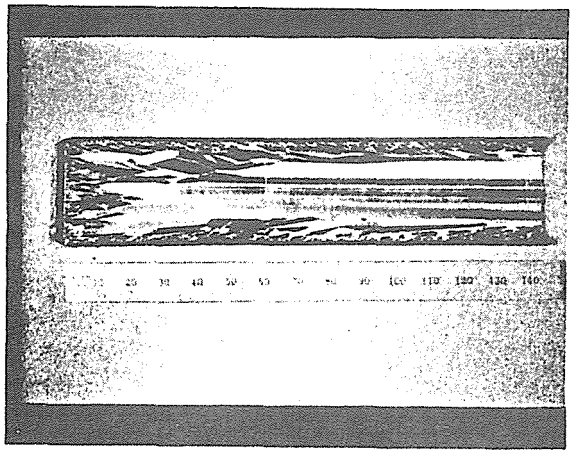

Fig. 1. Unseeded ESP Sheet Etched in NaOH to Reveal Grain Structure

process described in detail in reference (4). Semiconductor-grade silicon melts were used for sheet growth. All melts were doped with boron to yield approximately 1 Ω-cm, p-type silicon sheets. The filaments used were machined dense graphite rods 1.5 mm in diameter. The silicon sheets were grown unseeded; i.e., at the beginning of each sheet growth, a liquid meniscus is stabilized between two graphite filaments spaced 40 mm apart, and a graphite bridge joining the filaments. Pull speeds were 6 to 30 mm/min. In addition to pull speed, the sheet thickness is also affected by the hot zone temperature in the vertical quartz tube furnace (3). Faster speeds and/or higher hot zone temperatures produce thinner sheets and vice versa. The equilibrium grain structure of silicon sheets grown at our laboratory is normally reached within about 10 cm of growth from the graphite bridge.

Silicon sheets with average thicknesses from about 100 μm to 1100 μm were produced for our electron channeling and EBIC studies (6). Samples measuring about 1 cm by 4 cm (the width of the sheet) were cut from each silicon sheet at least 15 cm from the graphite bridge. For each sample, the grain orientations of all grains across the sheet width with grain widths larger than about 0.5 mm were determined from their electron channeling patterns. Except for the 1100-μm-thick sample, all the small grains ignored were within about 3 mm of the graphite filaments. Figure 2(a) shows the grain orientations determined for a sample obtained from an ESP silicon sheet with an average thickness of about 1100 μm. The pull speed during growth for this sheet was 8 mm/min. The location of the dots inside the stereographic projection unit triangle in Figure 2 indicates the direction of the surface normal of the grains. Grains separated by twin boundaries are treated as single grains in the figure. The linear angular scale of the unit triangle can be easily determined from the fact that the angle between the [001] pole and the [011] pole is 45°. The arrows plotted in Figure 2 indicate the grain growth direction during ribbon pulling. The grain growth direction in the center portion of ESP silicon sheets is normally 180° off the sheet pulling direction. The grain orientations shown in Figure 2(a) are primarily those of relatively short grains typical of very thick ESP silicon sheets. From Figure 2(a) it is obvious that the surface normals and grain growth directions of these grains are random. Figure 2(b) shows the grain orientations determined from a sample obtained from an ESP silicon sheet with an average thickness of about 480 μm. The pull speed during growth for this sheet was 12 mm/min. A close examination of the grains and the orientations of their surface normals revealed that grains with surface normals less than about 16° off the [011] direction occupy about three-quarters of the area of the center portion of the silicon sheet. Many of these grains are several millimeters wide with long linear grain boundaries several centimeters long and running

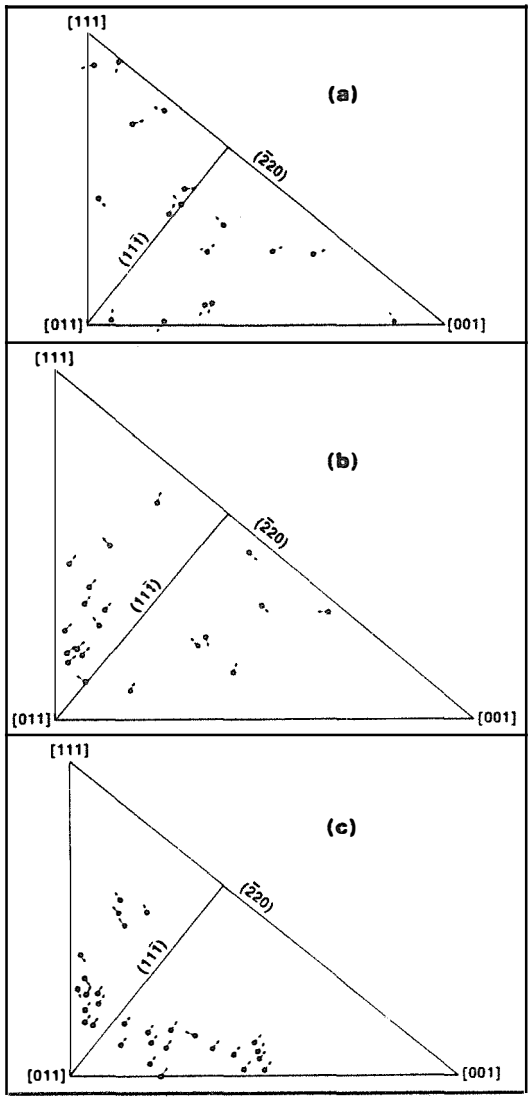

Fig. 2. Grain Orientations of ESP Silicon Sheets in Samples (a) 1100 μm Thick, (b) 480 μm Thick, and (c) 110 μm Thick

parallel to the graphite filaments. The plane that is parallel to the growth direction and perpendicular to the surfaces for these long grains with linear boundaries is very close to (11$\bar{1}$). This type of grain structure is often observed in ESP silicon sheets grown in our laboratory. Figure 2(c) shows the grain orientations determined for an even thinner sample obtained from an ESP silicon sheet with an average thickness of about 110 μm. The pull speed during growth for this sheet was 30 mm/min. The dominant grain structure is now quite obvious. All of the grains have surface normals less than 20° off the [011] direction; the plane that is parallel to the growth direction and perpendicular to the surfaces for three-quarters of the grains is very close to (111).

EBIC measurements were taken on the three samples whose grain orientations are shown in Figure 2. For the 480-μm-thick sample whose grain orientations are shown in Figure 2(b), we observed sharp variations in the intensity of EBIC signals from grain to grain, such as those shown in Figure 3. The darker grains in the EBIC images are caused by the higher density of points of emergence of the electrically active dislocations, which serve as recombination centers, at the grain surface. Correlation of the EBIC image intensities of the grains with the grain orientations showed that all the grains with bright EBIC images (i.e., grains with very low dislocation densities and thus higher short-circuit current densities) have their surface nromals oriented near [011]. The electrically active dislocation densities for such grains, determined by counting recombination centers in 100 magnification EBIC pictures, are less than 5×10^3 cm^{-2}. For grains with dark EBIC images, the electrically active dislocation densities are on the order of 2×10^5 cm^{-2} or more.

For the 1100-μm and 110-μm-thick samples, no significant variations in the intensity of EBIC signals from grain to grain were observed. However, the overall EBIC signal level observed for the 110-μm-thick sample is significantly higher

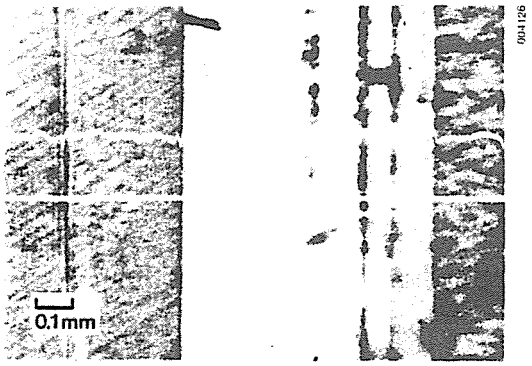

Fig. 3. EBIC Image and Line-Scan of Part of Sample (b) in Fig. 2 Taken at 35 keV Electron Beam Energy. The straight horizontal line in the picture indicates both the place where the line-scan was performed and the zero beam current reference.

than that of the thicker sample. Total defect densities, rather than only electrically active defect densities, of these two silicon sheets were studied using preferential chemical etching. For the 1100-μm-thick sheet, the dislocation density is high, on the order of 1×10^6 cm^{-2}, over most of the surface area. For the 110-μm sheet, the density of dislocation etch pits observed varies from essentially zero in some areas of the sheet up to about 3×10^5 cm^{-2}.

Our observation of the dominant grain structure in thinner ESP silicon sheets whose grain growth during unseeded sheet pulling has reached a steady-state condition is consistent with our past findings (3) that (a) very large grains can be achieved when a seed crystal is used with crystallographic orientations the same as those of our observed dominant grain structure in seeded ESP sheet growth, and (b) the (111) twin planes can block the propagation of spurious grains that nucleate at the filaments, which results in long, linear grains in the center of the silicon sheet.

LOW-ANGLE SILICON SHEETS

In the LASS growth process (7,8), a silicon sheet, typically 5 to 6 cm wide, is pulled almost horizontally from the melt which is contained in a shallow rectangular quartz crucible. The solid-liquid interface area in this process is significantly greater than it is in a vertical silicon sheet pulling process such as ESP. The efficient extraction of the latent heat of fusion in the LASS process makes possible very high linear growth rates--a linear growth rate of up to 80 cm/min (450 cm^2/min area growth rate) has been demonstrated. In addition to the high area productivity, the LASS process has excellent growth stability--continuous growths over one hour have been achieved (7). Three main types of structures have been found to occur in LASS material: random dendritic, parallel dendritic, and twin-stabilized planar growth. The random and parallel dendritic materials are polycrystalline with rough top surfaces composed of random or parallel dendrites. The twin-stabilized planar growth material has a much smoother top surface with parallel, faceted surface structures (less than 0.1 mm high) on the top. Figure 4 shows the top surface appearance of a twin-stabilized planar growth LASS material surrounded on three sides by random dendritic material. The bottom surface of a LASS sheet is generally quite smooth.

The twin-stabilized planar growth material was reported by EMC to be single-crystal except for a twin plane very near the top surface (8). We have studied twin-stabilized planar growth LASS in two different silicon sheets that we received from EMC. Our electron channeling study showed that the twin-stabilized planar growth material is essentially single-crystal with a surface normal close to [111] (Figure 5). The parallel, faceted structures on the top surface are running along the [$\bar{2}$11] direction. Optical and SEI micrographs of polished and then preferentially etched samples showed that the dislocation density varies from as

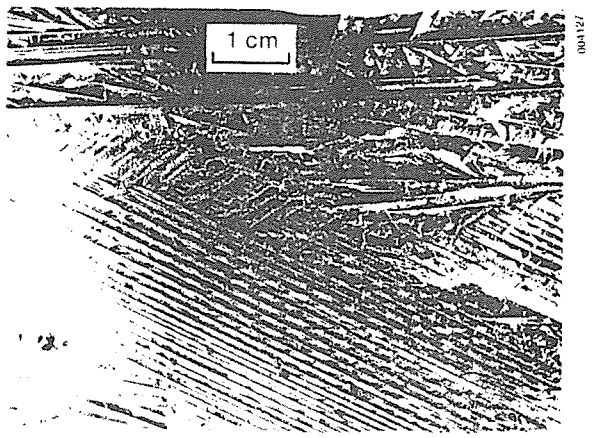

Fig. 4. Part of a LASS Silicon Sheet Showing Both the Random Dendritic Region and the Twin-Stabilized Planar Growth Region

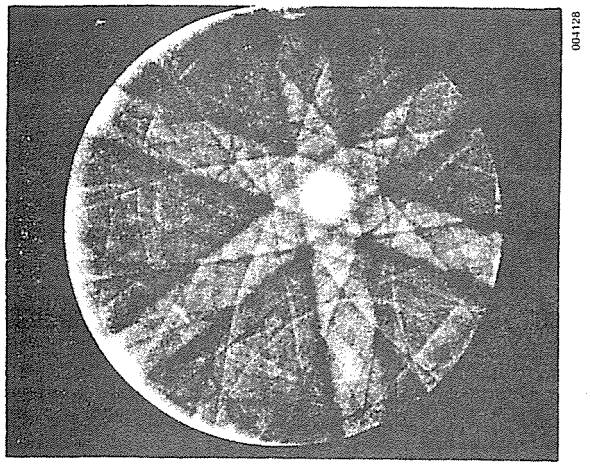

Fig. 5. The Electron Channeling Pattern of a Twin-Stabilized Planar Growth Region of a Low-Angle Silicon Sheet

low as about 10^3 cm^{-2} to very high densities in some areas of the material. Although we have never observed any twin boundaries, high densities of dislocations and stacking faults are often observed under the parallel, faceted surface structures. EBIC observations of electrically active dislocations are quantitatively similar to the optical and SEI observations. Figure 6 is an EBIC micrograph taken on a p-n junction solar cell fabricated on a polished LASS twin-stabilized growth sample showing the high density of electrically active dislocations existing under the parallel, faceted top surface structures. In addition to dislocations and stacking faults, we have also observed polycrystalline silicon islands and what appear to be large dislocation loops in the twin-stabilized planar growth material. They are normally less than 100 μm in diameter and less than about 3 cm^{-2} in density. They normally grow larger toward the bottom surface and penetrate through the entire sheet thickness. Their existence does not disrupt the single-crystal growth mechanism surrounding them.

Eleven solar cells 0.1 cm^2 in area and two solar cells 1.6 cm^2 in area have been fabricated on twin-stabilized growth LASS samples having 4 Ω-cm resistivity and polished to a thickness of about 250 μm. The AM1 efficiencies of these solar cells vary from about 10.0% (for a 1.6-cm^2 cell) to 12.7% (for a 0.1-cm^2 cell). A control cell 1.61 cm^2 in area fabricated on 2.5 Ω-cm Czochralski-grown (CZ) silicon has an AM1 efficiency of 14.8%. Minority carrier diffusion length (MCDL) measurements performed on the two large-area LASS solar cells showed that the base regions of the cells have a 16- and a 31-μm MCDL, respectively. The MCDL measured for the control CZ single-crystal silicon solar cell was 164 μm.

SUMMARY

We have studied the structural and electrical properties of silicon sheets grown by two different processes—ESP and LASS. We have found a dominant grain structure in thin ESP silicon sheets whose grain growth reached a steady-state condition after several centimeters of unseeded growth. That dominant grain structure consists of long grains with surface normals near the [011] direction. The plane that is parallel to the growth direction and perpendicular to the surfaces for most of these grains is very close to (111). We have also seen indications that grains with this dominant structure tend to have fewer electrically active dislocations than random grains. For the low-angle silicon sheets, we have studied the structure of the essentially single-crystal twin-stabilized planar growth material and have shown that although nearly dislocation-free areas do exist, most of the material has relatively high defect densities. This is consistent with the relatively low MCDL values we measured in this material. However, solar cells fabricated on such LASS substrates are reasonably good, having efficiencies between 65%

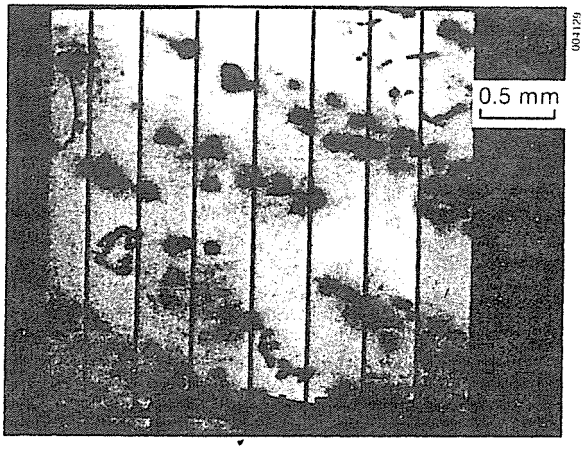

Fig. 6. EBIC Image of a Diffused p-n Junction LASS Solar Cell

and 85% of that of the control CZ silicon solar cell.

ACKNOWLEDGMENTS

This work was supported by the U.S. Department of Energy under Contract No. DE-AC02-83CH10093. The authors thank T. Ciszek and J. Hurd for supplying the ESP silicon sheets and many valuable suggestions, J. Milstein for helpful discussions, T. Schuyler for cell fabrication and measurements, and D. Jewett and H. Bates for supplying the LASS samples.

REFERENCES

1. D. C. Joy, D. E. Newbury, and D. L. Davidson, "Electron Channeling Patterns in the Scanning Electron Microscope," J. Appl. Phys., Vol. 53, pp. R81-R122, 1982.

2. H. J. Leamy, "Charge Collection Scanning Electron Microscopy," J. Appl. Phys., Vol. 53, R51-R80, 1982.

3. T. F. Ciszek and J. L. Hurd, "Melt Growth of Silicon Sheets by Edge-Supported Pulling," Proc. of Symp. Electronic and Optical Properties of Polycrystalline or Impure Semiconductors and Novel Silicon Growth Methods, K. V. Ravi and B. O'Mara, eds., The Electrochemical Society, Inc., Pennington, New Jersey, pp. 213-222, 1980.

4. J. L. Hurd and T. F. Ciszek, "Semicontinuous Edge-Supported Pulling of Silicon Sheets," J. Cryst. Growth, Vol. 59, pp. 499-506, 1982.

5. T. F. Ciszek, J. L. Hurd, and M. Schietzelt, "Filament Materials for Edge-Supported Pulling of Silicon Sheet Crystals," J. Electrochem. Soc., Vol. 129, pp. 2838-2843, 1982.

6. Y. S. Tsuo, J. L. Hurd, R. J. Matson, and T. F. Ciszek, "Electron Channeling and EBIC Studies of Edge-Supported Pulling Silicon Sheets," to be published in IEEE Transactions on Electron Devices, May 1984.

7. D. N. Jewett, H. E. Bates, and J. W. Locher, "Progress in Growth of Silicon Ribbon by a Low Angle, High Rate Process," Proceedings of Sixteenth IEEE Photovoltaic Specialists Conference, pp. 86-89, 1982.

8. D. N. Jewett, Proceedings of SERI Annual Polycrystalline Silicon Solar Cells Subcontractors' Review Meeting, Golden, Colorado, June 27-28, 1983.